Redox Tuning via Ligand-Induced Geometric Distortions at a YMn_3O_4 Cubane Model of the Biological Oxygen Evolving Complex

Heui Beom Lee† and Theodor Agapie*†

† Department of Chemistry and Chemical Engineering, California Institute of Technology, 1200 E California Blvd MC 127-72, Pasadena, CA 91125, USA

Supporting information

Experimental procedures

General considerations

All reactions were performed at room temperature in an N_2-filled glovebox or by using standard Schlenk techniques unless otherwise specified. Glassware was oven dried at 150 °C for at least 2h prior to use, and allowed to cool under vacuum. All reagents were used as received unless otherwise stated. Anhydrous tetrahydrofuran (THF) was purchased from Aldrich in 18 L Pure-Pac™ containers. Anhydrous CH_2Cl_2, CH_3CN, diethyl ether, benzene and THF were purified by sparging with nitrogen for 15 minutes and then passing under nitrogen pressure through a column of activated A2 alumina. NMR solvents were purchased from Cambridge Isotope Laboratories, dried over calcium hydride, degassed by three freeze-pump-thaw cycles and vacuum-transferred prior to use. Paramagnetic ^{1}H NMR spectra were recorded on a Varian 300 MHz instrument, with shifts reported relative to the residual solvent peak. Elemental analyses were performed at the California Institute of Technology.

Synthesis of H_3triam

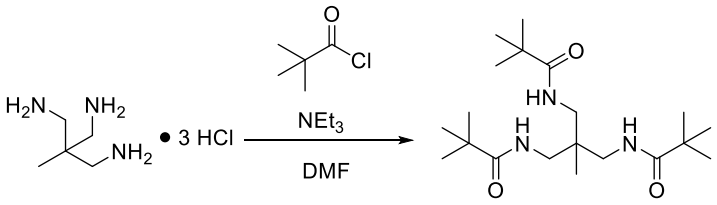

Prepared according to literature[1], the HCl salt of 1,1,1-tris(aminomethyl)ethane (1.5 g, 6.62 mmol, 1 equiv) was suspended in DMF (100 mL) and treated with Et_3N (10 mL). The resulting mixture was cooled to 0 °C in an ice bath then treated with pivaloyl chloride (5 mL) dropwise. The mixture was warmed to room temperature and stirred for 2 days at room temperature. All volatiles were removed under reduced pressure, and the residue was treated with CH_2Cl_2 and saturated aqueous $NaHCO_3$. The CH_2Cl_2 layer was separated, washed with water, dried over anhydrous $MgSO_4$, and filtered. All volatiles were removed from the filtrate, and the residue was washed with copious amounts of Et_2O. H_3triam was obtained was an off-white powder. Yield: 750 mg, 31 %.

^{1}H NMR (500 MHz, $CDCl_3$): δ 7.09 (t, J = 5 Hz, 3H, N*H*), 2.90 (d, J = 5 Hz, 6H, C*H*$_2$), 1.24 (s, 27H, −C(C*H*$_3$)$_3$), 0.77 (s, 3H, C*H*$_3$) ppm.

^{13}C NMR (125.7 MHz, $CDCl_3$): 180.12, 42.25, 41.48, 39.04, 27.85, 19.27 ppm.

HRMS (FAB+): calcd. For $C_{20}H_{40}N_3O_3$: 370.3070; found: 370.3059 [M+H]

Synthesis of **4-Mn**

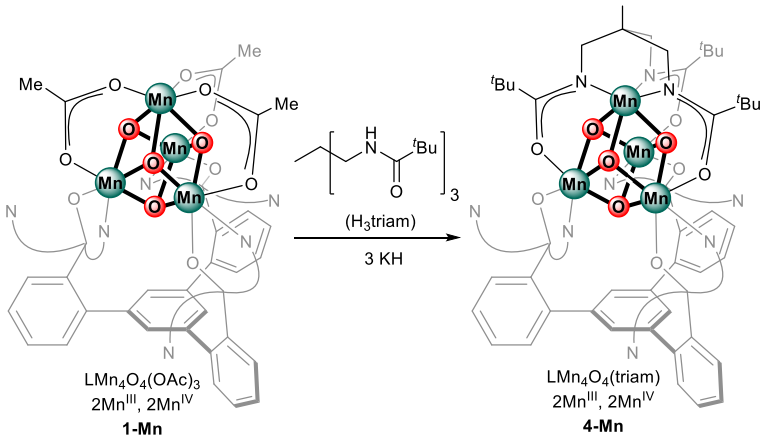

A solution of H_3triam (265 mg, 0.717 mmol, 1.1 equiv) in THF (200 mL) was treated with KH (300 mg, ~10 equiv) and stirred for 18 hours at room temperature. Excess KH was removed by filtration, and the filtrate was treated with **1-Mn** (860 mg, 0.653 mmol, 1 equiv). After stirring for 18 hours at room temperature, all volatiles were removed from the crude reaction mixture. The residue was washed with generous amounts of Et_2O and benzene, then redissolved in CH_2Cl_2 and filtered through a pad of Celite. All volatiles were removed from the filtrate. The residue was washed three times with small amounts of MeCN, redissolved in CH_2Cl_2 and filtered through a pad of Celite. Volatiles were removed from the filtrate under reduced pressure, yielding **4-Mn** as a brown powder. Yield: 820 mg, 83 %. Crystals suitable for X-ray crystallography were obtained from slow vapor diffusion of Et_2O into a concentrated solution of **4-Mn** in CH_2Cl_2. ^{1}H NMR (300 MHz, CD_2Cl_2): δ 35.5, 30.0, 17.8, 13.3, 9.7, −5.9 ppm.

Synthesis of **4-Mn-ox**

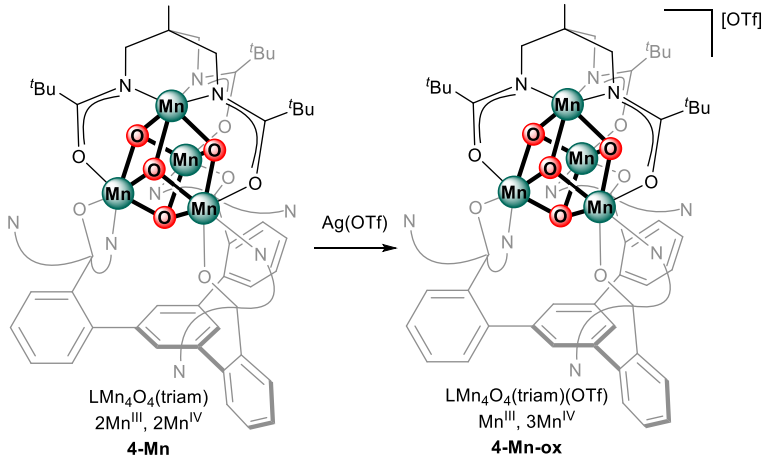

A solution of **4-Mn** (220 mg, 0.146 mmol, 1 equiv) in THF (10 mL) was treated with a solution of Ag(OTf) (40 mg, 0.155 mmol, 1.05 equiv) in MeCN (3 mL) and stirred for 18 hrs at room temperature. All volatiles were removed from the crude reaction mixture. The residue was washed with generous amounts of Et_2O and ben. The residue was dissolved in CH_2Cl_2 and filtered through a pad of Celite. All volatiles were removed from the filtrate. The residue was washed three times with small amounts of THF, redissolved in CH_2Cl_2 and filtered through a pad of Celite. Volatiles were removed from the filtrate under reduced pressure, yielding **4-Mn-ox** as a brown powder. Yield: 133 mg, 55 %. Crystals of **4-Mn-ox** suitable for EPR spectroscopy were obtained from slow vapor diffusion of Et_2O into a concentrated solution in CH_2Cl_2. ^{1}H NMR (300 MHz, CD_2Cl_2): δ 114.5, 74.6, 13.1, 11.0, −18.5 ppm. Analysis calculated for [LMn_4O_4(triam)](OTf) [$C_{78}H_{75}F_3Mn_4N_9O_{13}S$]: C 56.60, H 4.57, N 7.62; found: C 56.34, H 4.46, N 7.97.

Synthesis of **2-Y**

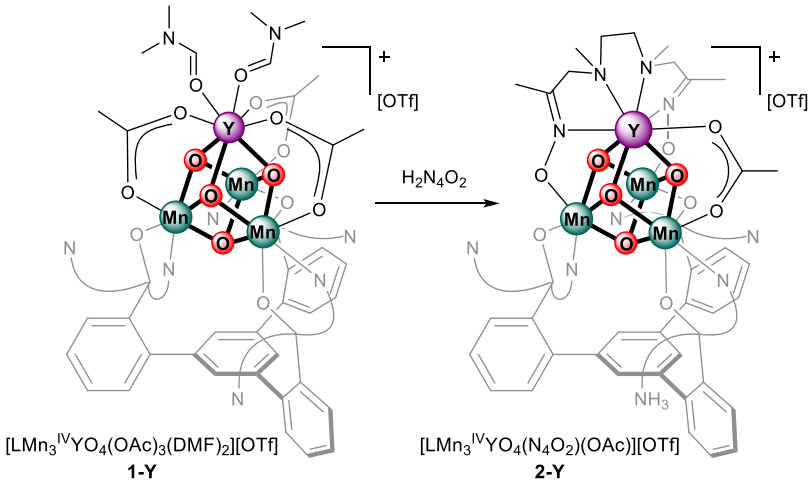

$[LMn_3^{IV}YO_4(OAc)_3(DMF)_2][OTf]$ **1-Y**

$[LMn_3^{IV}YO_4(N_4O_2)(OAc)][OTf]$ **2-Y**

A solid mixture of **1-Y** (930 mg, 0.565 mmol, 1 equiv) and $H_2N_4O_2$ (143 mg, 0.62 mmol, 1.1 equiv) was treated with THF (18 mL) and stirred at room temperature for 16 hours. The resulting red precipitate was collected, washed with THF until the filtrate was no longer red, dissolved in CH_2Cl_2, and filtered through Celite. Volatiles were removed from the filtrate under reduced pressure, yielding **2-Y** as a red powder. Crystals suitable for X-ray crystallography were obtained from slow vapor diffusion of Et_2O into a concentrated solution of **2-Y** in py (250 mg, 26%). ^{1}H NMR (300 MHz, CD_2Cl_2): δ 68.2, 61.2, 18.6, 17.1, 11.8, 11.0, −17.0, 19.2 ppm. Analysis calculated for $[LYMn_3O_4(N_4O_2)(OAc)(DMF)](OTf)$ $[C_{73}H_{69}F_3Mn_3N_{11}O_{15}SY]$: C 52.09, H 4.13, N 9.15; found: C 52.07, H 4.23, N 9.37.

Synthesis of **3-Y-red**

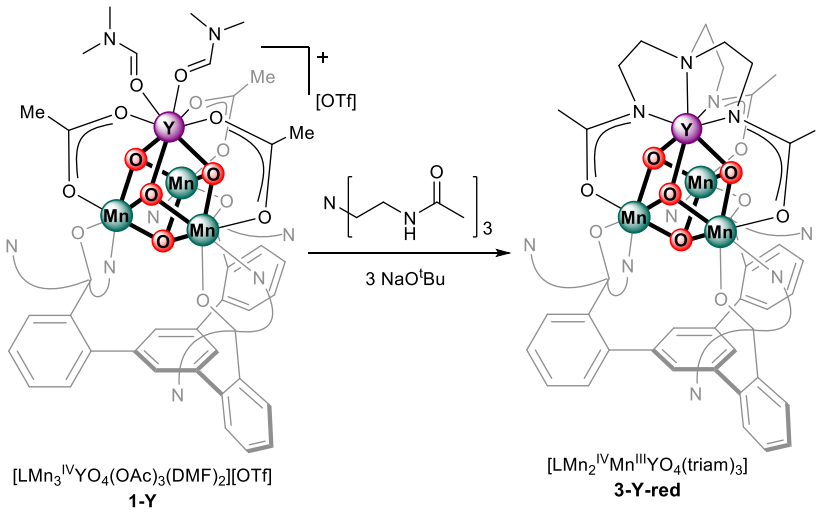

A solid mixture of **1-Y** (420 mg, 0.255 mmol, 1 equiv) and the triacetamide (85 mg, 0.312 mmol, 1.2 equiv) was treated with MeCN (18 mL) and stirred briefly at room temperature. NaO^{t}Bu (81 mg, 0.843 mmol, 3.3 equiv) was added as a solid and the mixture was stirred at room temperature for 16 hours. The resulting orange-brown precipitate was collected, washed with MeCN until the filtrate was no longer brown, dissolved in CH_2Cl_2, and filtered through Celite. Volatiles were removed from the filtrate under reduced pressure, yielding **3-Y-red** as a red powder. (120 mg, 32%). ^{1}H NMR (300 MHz, CD_2Cl_2): δ 24.9, 11.2, 10.2, 9.3, −22.43 ppm.

Synthesis of **3-Y**

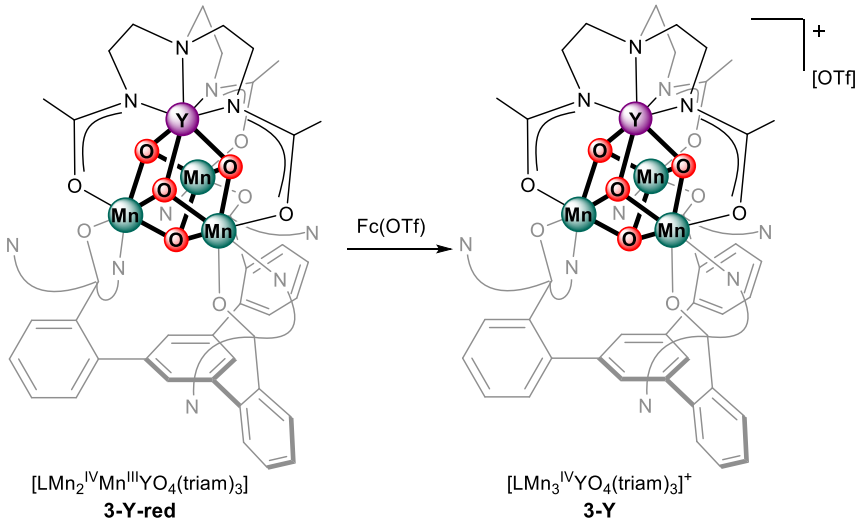

A solution of **3-Y-red** (28 mg, 0.019 mmol, 1 equiv) in CH_2Cl_2 (3 mL) was treated with a solution of Fc(OTf) (8 mg, 0.024 mmol, 1.2 equiv) in CH_2Cl_2 (2 mL). The mixture was stirred at room temperature for 16 hours. All volatiles were removed from the resulting red-brown solution, and the residue was washed with Et_2O. The residue was dissolved in cold THF (−30 °C) and filtered through a pad of Celite. Volatiles were removed from the filtrate under reduced pressure, yielding **3-Y** as a red powder. Yield: 28 mg, 90%. Crystals suitable for X-ray crystallography were obtained from slow vapor diffusion of Et_2O into a concentrated solution of **3-Y** in THF. ^{1}H NMR (300 MHz, CD_2Cl_2): δ 15.0, 11.5, 9.2, −15.4, −17.2 ppm. Analysis calculated for [LYMn$_3$O$_4$(Ntriam)](OTf)·CH_2Cl_2 [$C_{71}H_{62}Cl_2F_3Mn_3N_{10}O_{13}SY$]: C 50.85, H 3.73, N 8.35; found: C 50.56, H 4.02, N 8.09.

NMR spectroscopy

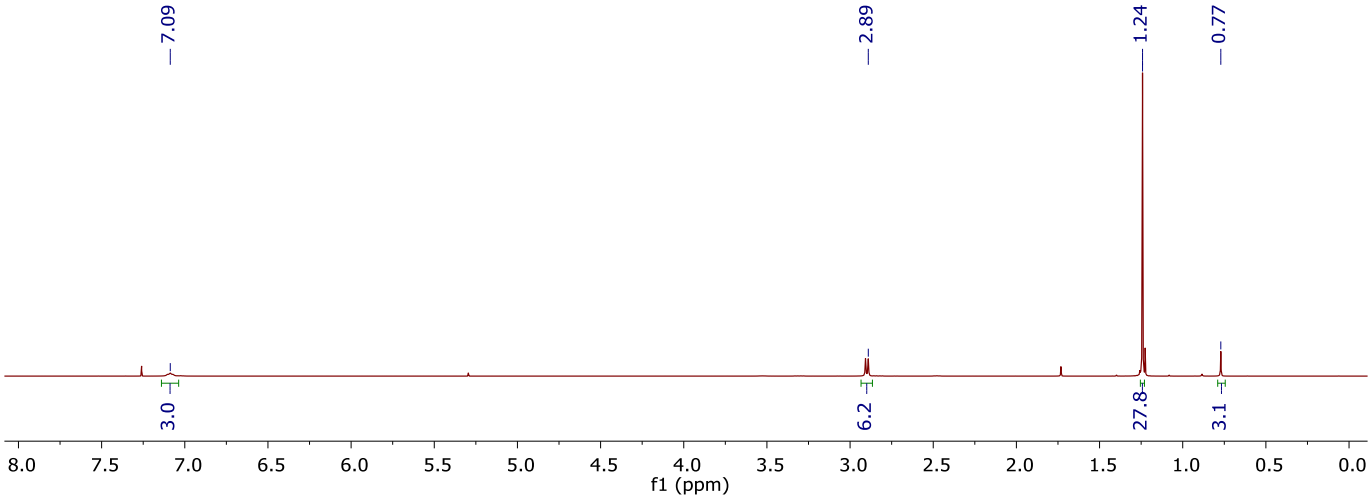

Figure S1. ^{1}H NMR of H_3triam in $CDCl_3$.

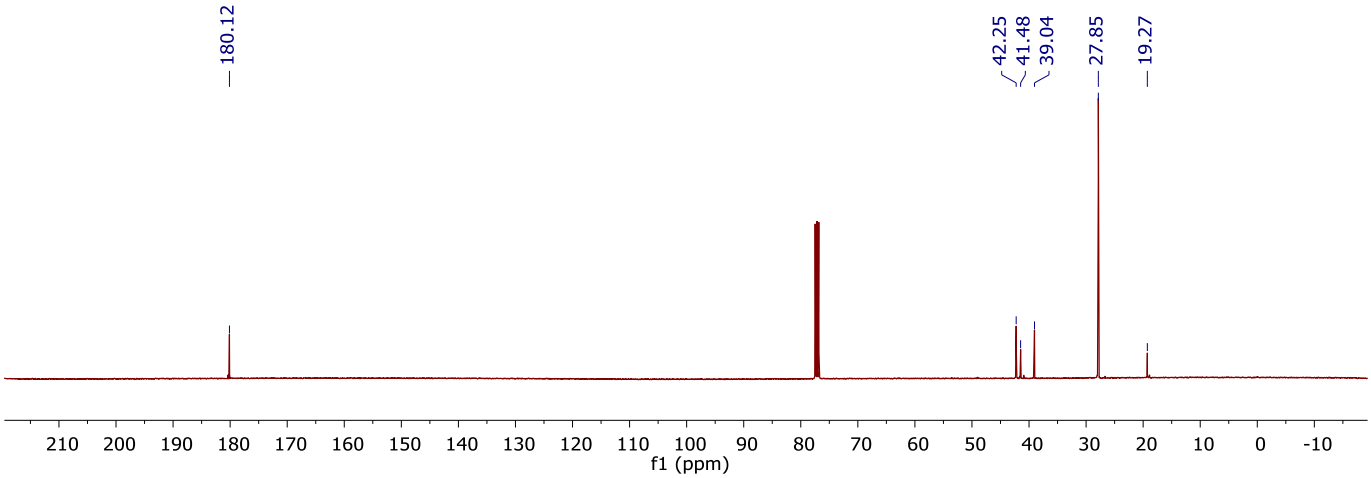

Figure S2. ^{13}C NMR of H_3triam in $CDCl_3$.

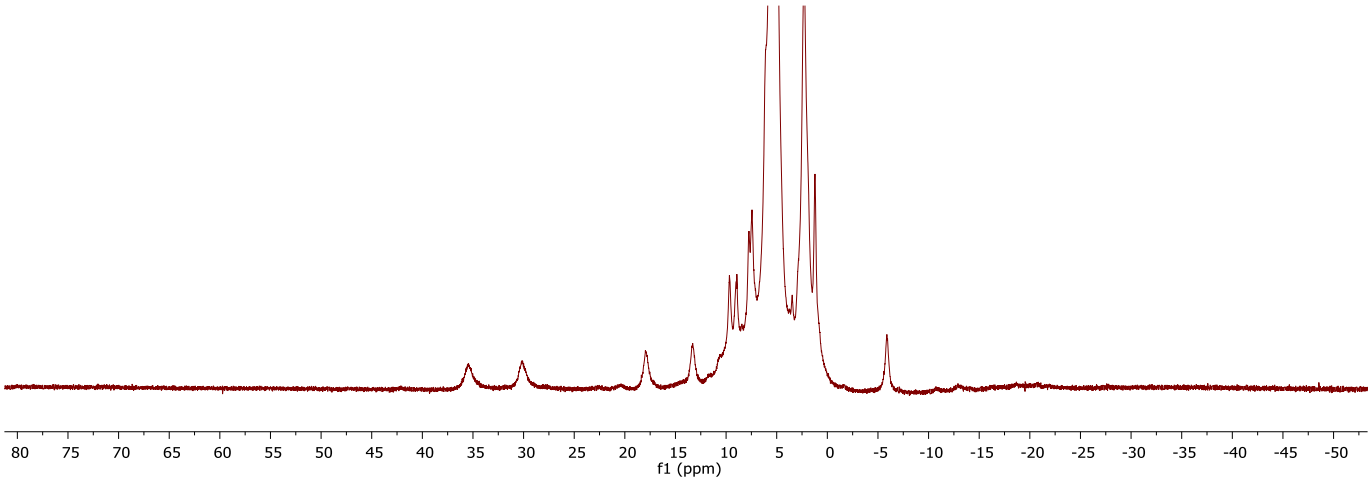

Figure S3. ^{1}H NMR of **4-Mn** in CD_2Cl_2.

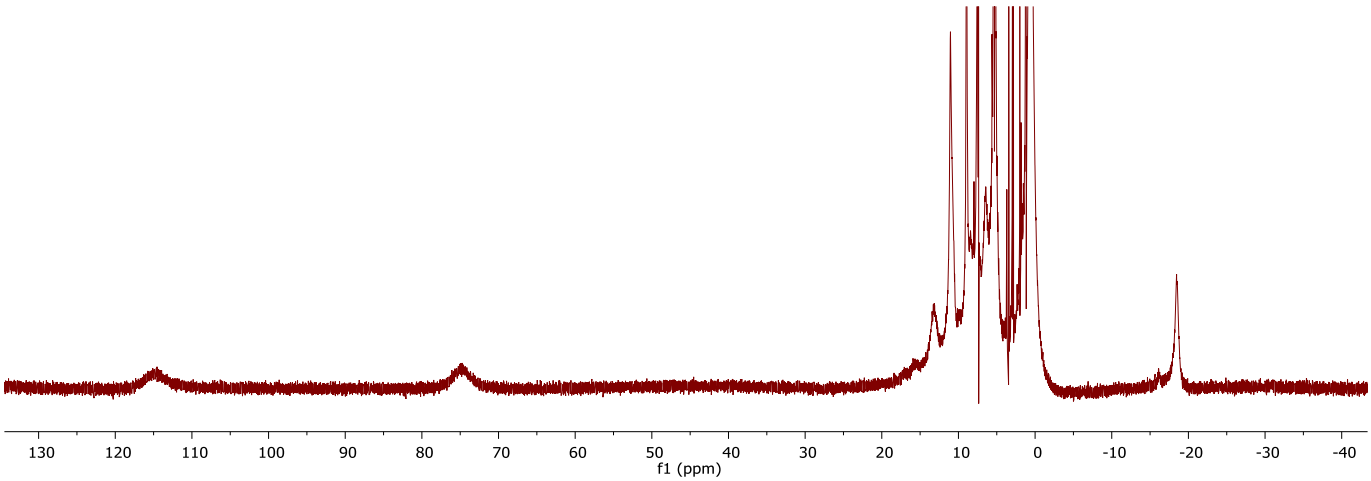

Figure S4. ^{1}H NMR of **4-Mn-ox** in CD_2Cl_2.

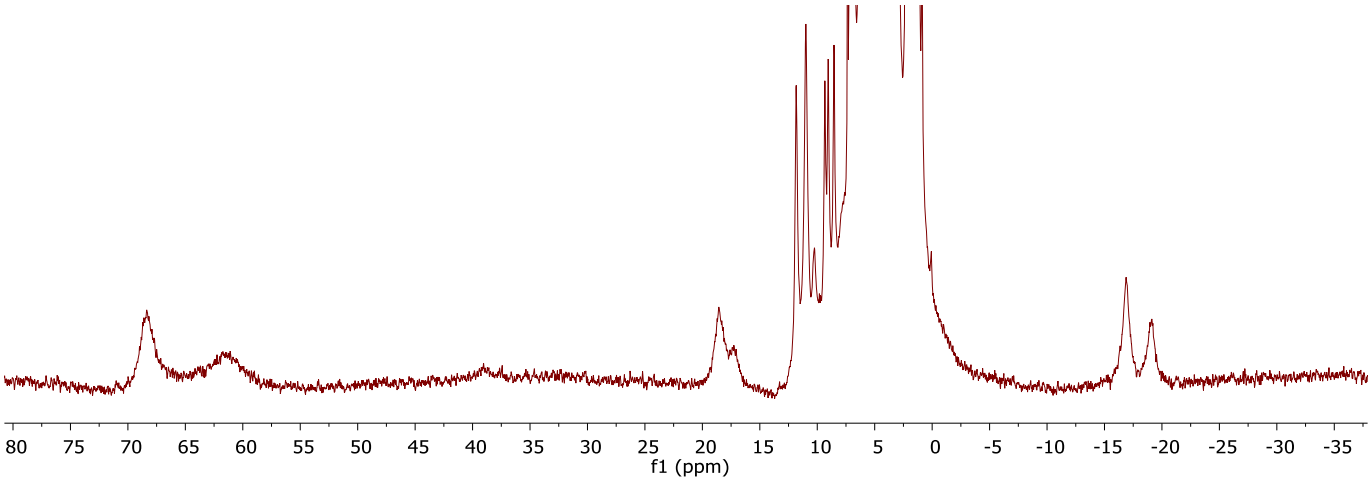

Figure S5. ^{1}H NMR of **2-Y** in CD_2Cl_2.

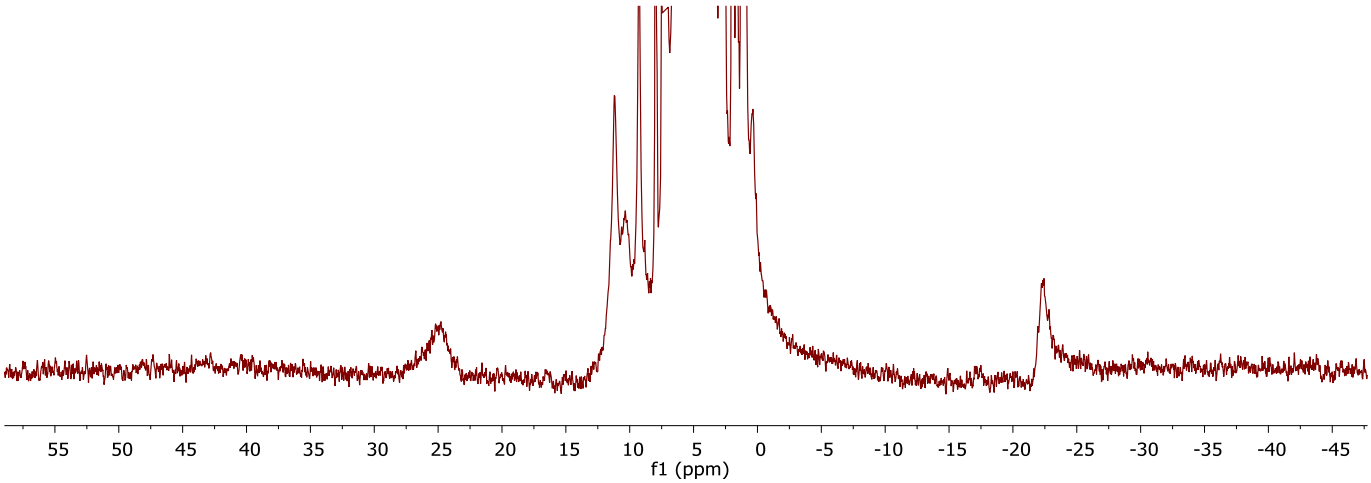

Figure S6. ^{1}H NMR of **3-Y-red** in CD_2Cl_2.

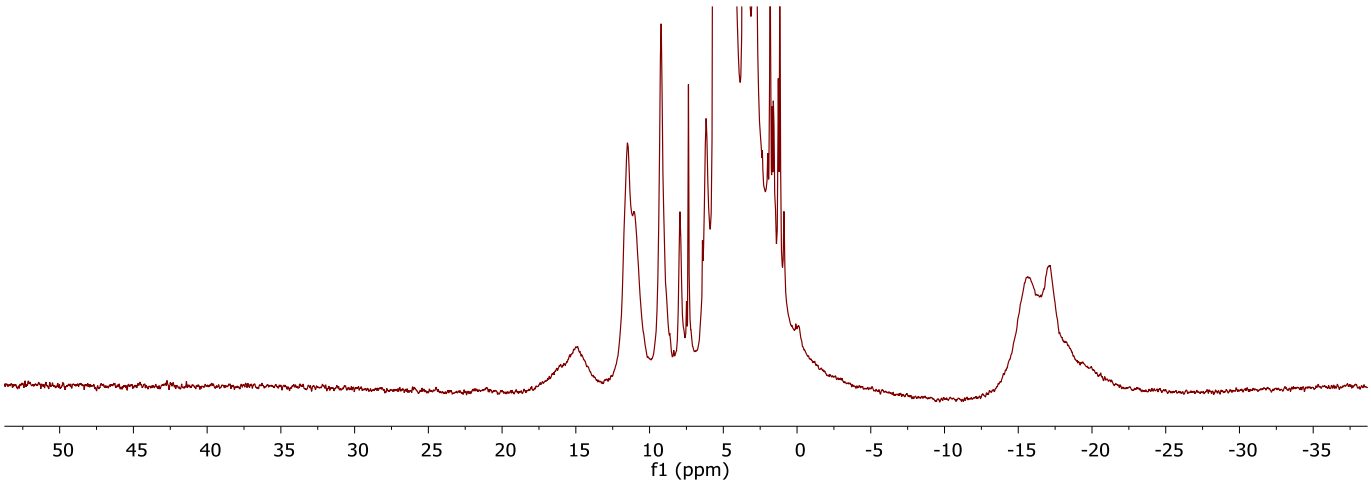

Figure S7. ^{1}H NMR of **3-Y** in CD_2Cl_2.

Electrospray mass spectrometry

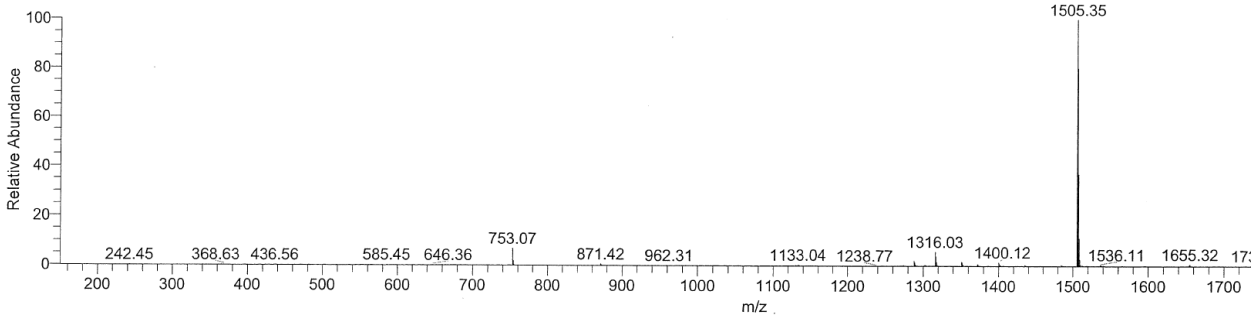

Figure S8. ESI-MS of **4-Mn**. *m*/*z* = 1505 consistent with $[LMn_4O_4(triam)]^+$.

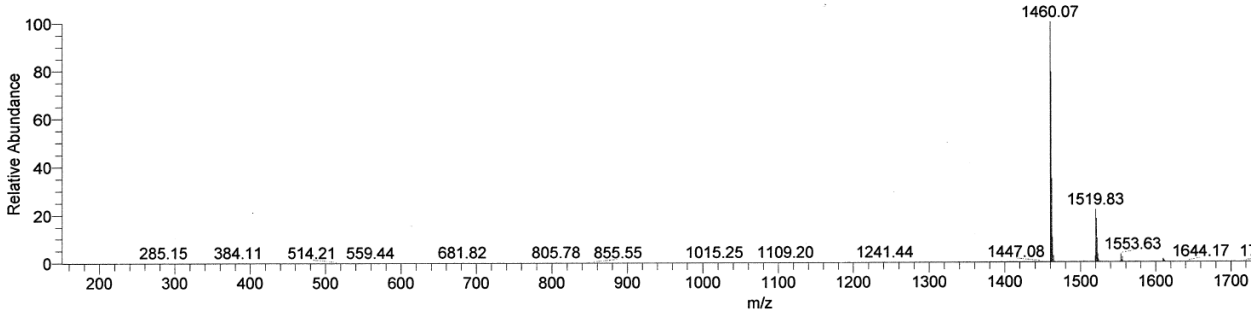

Figure S9. ESI-MS of **2-Y**. *m*/*z* = 1460 consistent with $[LYMn_3O_4(N_4O_2)(OAc)]^+$.

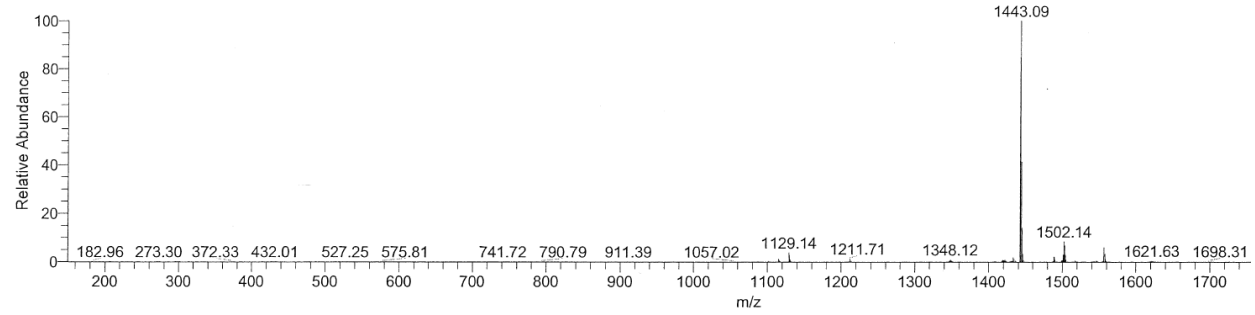

Figure S10. ESI-MS of **3-Y**. *m*/*z* = 1443 consistent with $[LYMn_3O_4(Ntriam)]^+$.

X-ray crystallography

Suitable crystals were mounted on a nylon loop using Paratone oil, then placed on a diffractometer under a nitrogen stream. X-ray intensity data were collected on a Bruker D8 VENTURE Kappa Duo PHOTON 100 CMOS detector employing Mo-Kα or Cu-Kα radiation (λ = 0.71073 Å or 1.54178 Å respectively) at a temperature of 100 K. All diffractometer manipulations, including data collection, integration and scaling were carried out using the Bruker APEX3 software. Frames were integrated using SAINT. The intensity data were corrected for Lorentz and polarization effects and for absorption using SADABS. Space groups were determined on the basis of systematic absences and intensity statistics using XPREP. Using Olex2, the structures were solved by direct methods using ShelXT and refined to convergence by full-matrix least squares minimization using ShelXL. All non-solvent non-hydrogen atoms were refined using anisotropic displacement parameters. Hydrogen atoms were placed in idealized positions and refined using a riding model. Graphical representation of structures with 50% probability thermal ellipsoids was generated using Diamond visualization software. Two component twin refinement for **4-Mn**.

Table S1. Crystal and refinement data for complexes **4-Mn**, **2-Y**, and **3-Y**.

Compound	**4-Mn**	**2-Y**	**3-Y**
CCDC	1897119	1897117	1897118
Empirical formula	$C_{81}H_{85}Mn_4N_9O_{12}$	$C_{92.48}H_{88.48}F_3Mn_3N_{14.9}O_{15}SY$	$C_{82}H_{60}F_3Mn_3N_{10}O_{16}SY$
Formula weight	1596.33	1991.34	1784.19
Temperature/K	100.0	100.0	99.99
Crystal system	triclinic	triclinic	monoclinic
Space group	P-1	P-1	C2/c
a/Å	12.1663(5)	13.9021(6)	25.8213(17)
b/Å	15.8988(7)	16.1176(7)	17.6106(12)
c/Å	21.2417(10)	21.2112(8)	35.578(2)
α/°	85.786(3)	87.635(3)	90
β/°	85.114(3)	77.947(3)	103.105(2)
γ/°	72.129(2)	83.333(3)	90
Volume/Å^3	3891.5(3)	4615.8(3)	15757.0(18)
Z	2	2	8
ρ_{calc}g/cm^3	1.362	1.433	1.504
μ/mm^{-1}	5.702	4.943	1.307
F(000)	1660.0	2049.0	7256.0
Crystal size/mm^3	0.5 × 0.5 × 0.1	0.1 × 0.1 × 0.05	0.1 × 0.1 × 0.1
Radiation	CuKα (λ = 1.54178)	CuKα (λ = 1.54178)	MoKα (λ = 0.71073)
2Θ range for data collection/°	5.848 to 150.194	7.034 to 149.336	4.412 to 54.95
Index ranges	-15 ≤ h ≤ 15, -19 ≤ k ≤ 19, 0 ≤ l ≤ 26	-17 ≤ h ≤ 17, -20 ≤ k ≤ 20, -26 ≤ l ≤ 26	-33 ≤ h ≤ 33, -22 ≤ k ≤ 22, -46 ≤ l ≤ 45
Reflections collected	13231	101142	125697
Independent reflections	13231 [R_{int} = merged, R_{sigma} = 0.0974]	18768 [R_{int} = 0.0560, R_{sigma} = 0.0428]	18015 [R_{int} = 0.0634, R_{sigma} = 0.0390]
Data/restraints/parameters	13231/2139/943	18768/0/1065	18015/49/942
Goodness-of-fit on F^2	1.072	1.055	1.061
Final R indexes [I>=2σ (I)]	R_1 = 0.1746, wR_2 = 0.4017	R_1 = 0.0624, wR_2 = 0.1781	R_1 = 0.0905, wR_2 = 0.2546
Final R indexes [all data]	R_1 = 0.2030, wR_2 = 0.4246	R_1 = 0.0695, wR_2 = 0.1842	R_1 = 0.1204, wR_2 = 0.2849
Largest diff. peak/hole / e Å^{-3}	3.46/-1.42	1.99/-2.23	3.20/-1.12

Table S2. Mn-oxo and Mn-Mn distances (Å) in complexes **1-Mn**, **2-Mn**, and **4-Mn**. Average distances underlined for emphasis.

	1-Mn	**2-Mn**	**4-Mn**
Mn(1)-O(1)	2.233(2)	1.883(2)	1.88(1)
Mn(1)-O(2)	2.012(2)	1.889(2)	1.92(2)
Mn(1)-O(3)	1.862(2)	2.007(3)	1.89(1)
Mn(2)-O(1)	1.869(2)	1.877(2)	1.92(1)
Mn(2)-O(3)	1.877(2)	1.868(2)	2.01(2)
Mn(2)-O(4)	1.847(2)	1.860(2)	1.98(1)
Mn(3)-O(2)	1.994(2)	1.908(2)	1.89(1)
Mn(3)-O(3)	1.848(2)	2.087(2)	1.98(1)
Mn(3)-O(4)	1.936(2)	1.879(2)	2.14(2)
Mn(4)-O(1)	1.898(2)	2.033(2)	1.92(2)
Mn(4)-O(2)	2.201(2)	1.977(2)	1.88(1)
Mn(4)-O(3)	1.937(2)	2.037(2)	1.85(1)
Mn-O average	1.960(2)	1.942(2)	1.94(1)
Mn(1)-Mn(2)	3.0724(6)	2.8997(6)	2.889(5)
Mn(1)-Mn(3)	2.9921(6)	2.9886(7)	3.008(4)
Mn(2)-Mn(3)	2.9174(6)	2.9021(7)	2.992(5)
Mn(1)-Mn(4)	2.9134(6)	2.8275(6)	2.783(4)
Mn(2)-Mn(4)	2.7663(6)	2.8307(6)	2.823(5)
Mn(3)-Mn(4)	2.8809(6)	2.8401(8)	2.797(4)
Mn-Mn average	2.9238(6)	2.8814(7)	2.882(5)

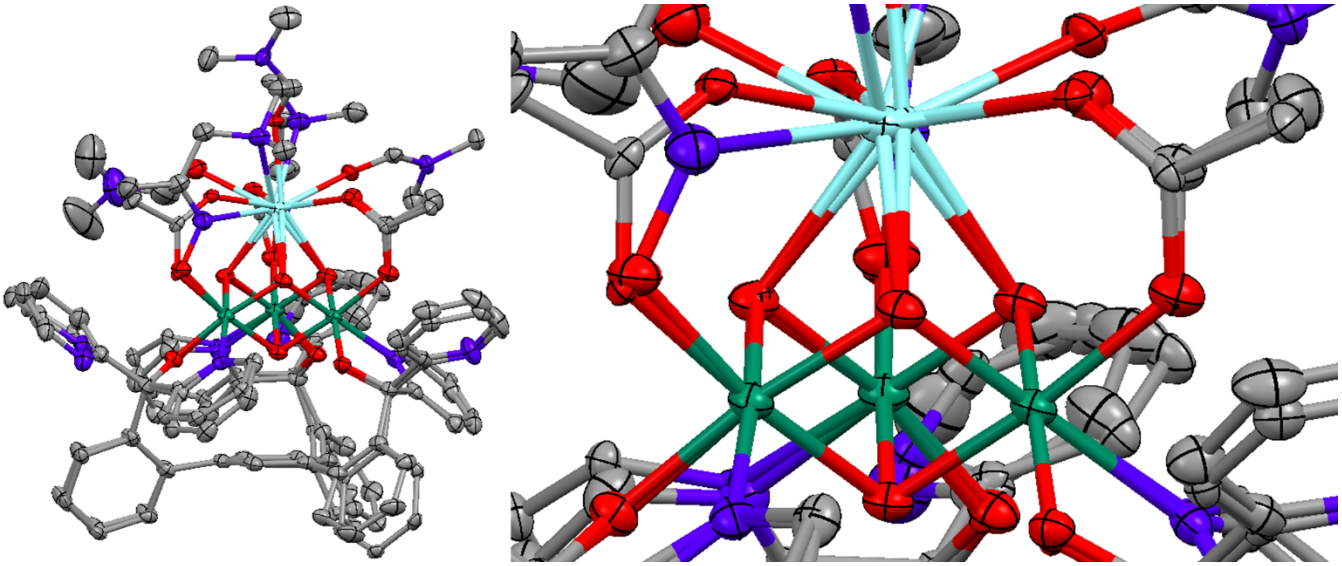

Figure S11. Overlay of the structures of **1-Y** and **2-Y**. The planes defined by the three Mn centers in each complex were fixed together. (Left) Full structure. (Right) Zoom-in of the [YMn_3O_4] core. The good overlap of the bridging acetate moieties in both complexes indicates a small change in Y-oxo/Y-Mn distances.

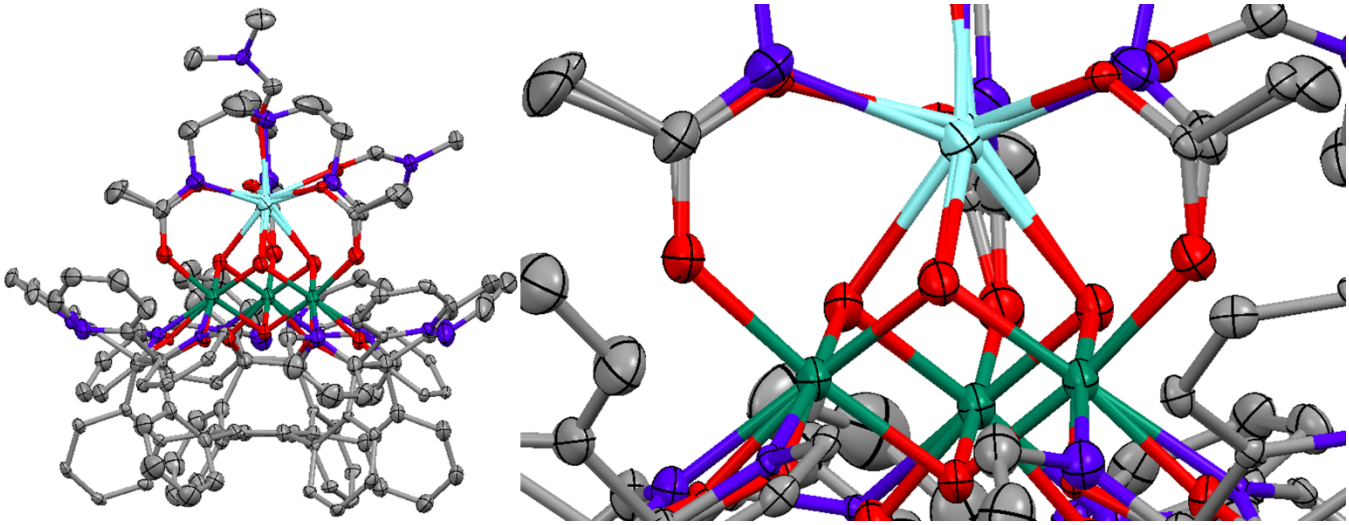

Figure S12. Overlay of the structure of **1-Y** and **3-Y**. The planes defined by the three Mn centers in each complex were fixed together. (Left) Full structure. (Right) Zoom-in of the [YMn_3O_4] core. The wider Y-O(acetate)-C(acetate) angles [126.8(2), 128.7(2), 136.1(2)] compared to the Y-N(amidate)-C(amidate) angles [124.4(5), 124.7(5), 125.1(4)] indicate a contraction in Y-oxo/Y-Mn distances in **3-Y** compared to **1-Y**.

Electrochemistry

Measurements were performed under an inert N_2 atmosphere in the glovebox using a Pine Instrument Company AFCBP1 bipotentiostat using the AfterMath software package. Cyclic voltammograms were recorded on 1.0 mM solutions of the relevant complex in the glovebox at 20 °C with an auxiliary Pt-coil counter electrode, Ag-wire reference electrode, and 3.0 mm glassy carbon working electrode (BASI). The electrolyte solution was 0.1 M [^{n}Bu$_4$N][PF$_6$] in dimethyl formamide. All reported values are referenced to an internal ferrocene/ferrocenium couple. Square-wave voltammograms were recorded using the following experimental parameters: amplitude 0.1 V, period 1 s, increment 10 mV, sampling width 1 ms. Peak cathodic and anodic currents from cyclic voltammograms at variable scan rates were plotted against the square root of the scan rate and fitted to a line.

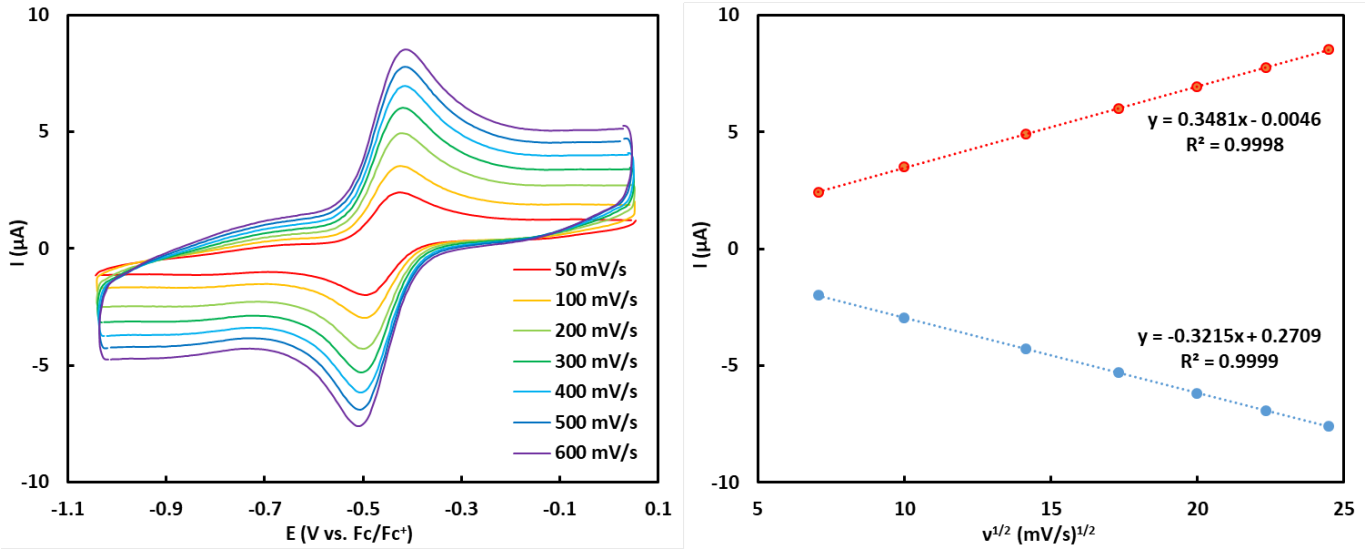

Figure S13. Cyclic voltammogram of **4-Mn** at various scan rates and plot of peak current vs. square root of scan rate.

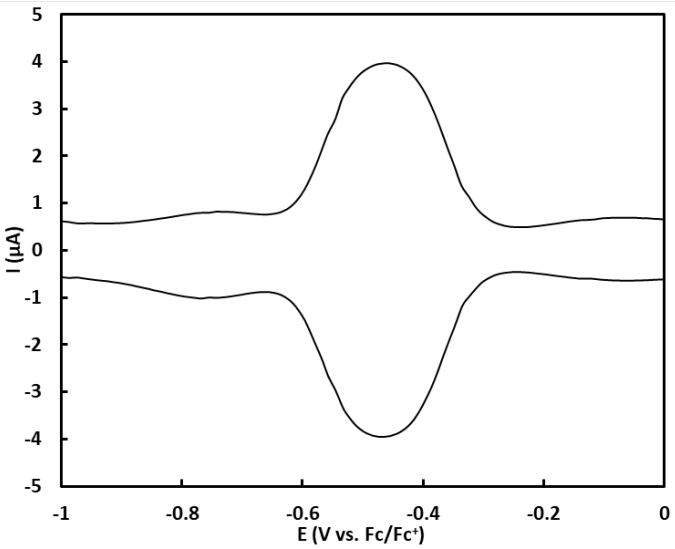

Figure S14. Square-wave voltammogram of **4-Mn**.

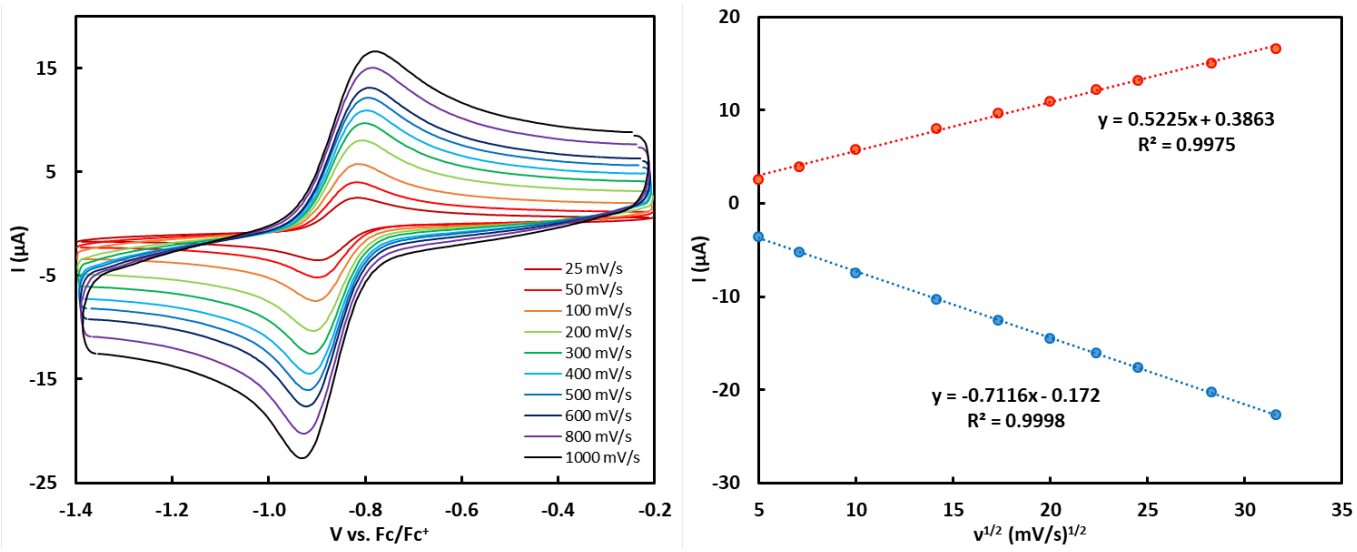

Figure S15. Cyclic voltammogram of **2-Y** at various scan rates and plot of peak current vs. square root of scan rate.

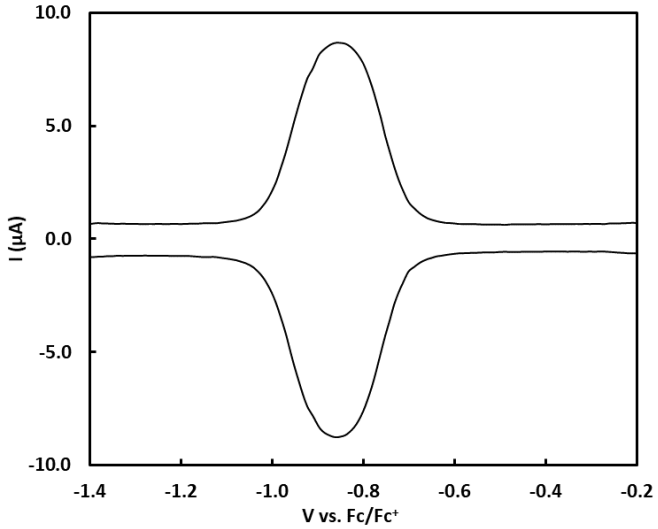

Figure S16. Square-wave voltammogram of **2-Y**.

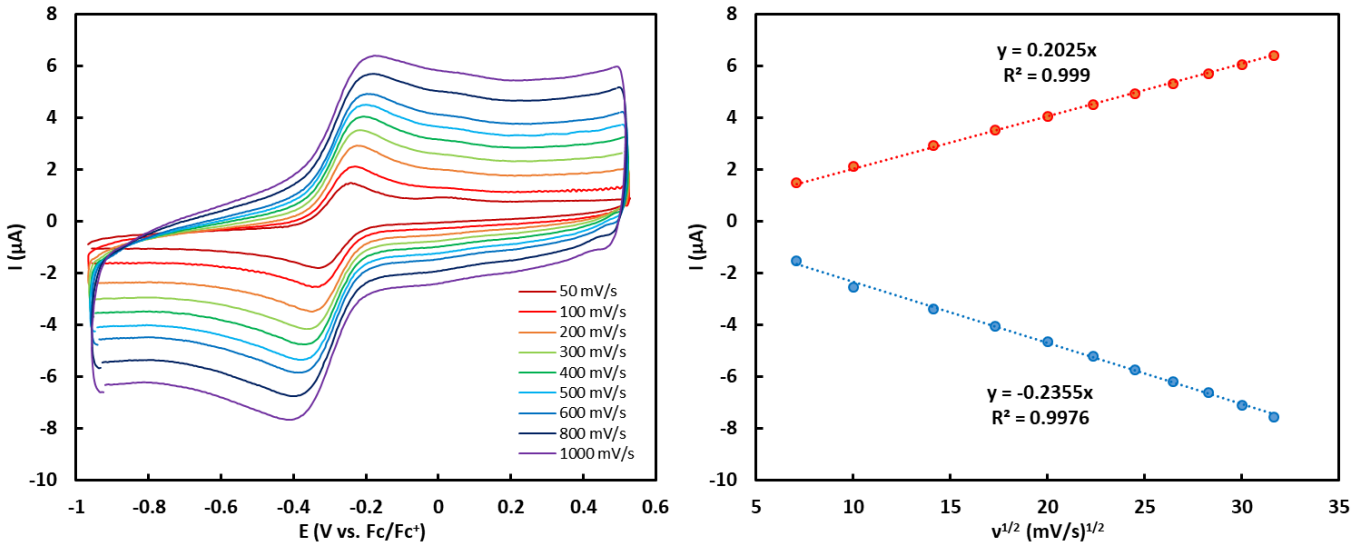

Figure S17. Cyclic voltammogram of **3-Y** at various scan rates and plot of peak current vs. square root of scan rate.

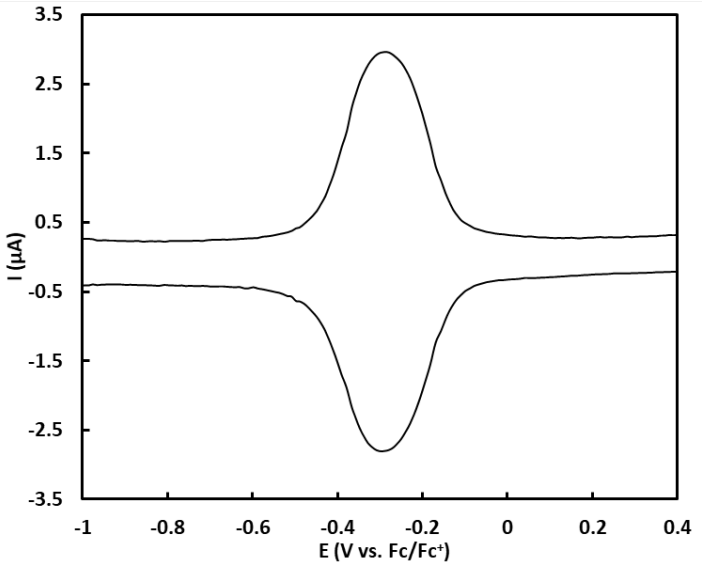

Figure S18. Square-wave voltammogram of **3-Y**.

Table S3. Values of ligand pK_a in DMSO, effective basicity, and cluster redox potential.

Complex	Ligand 1	Ligand 2	pKa ligand 1	pKa ligand 2	Effective basicity	Redox potential (V vs. Fc/Fc^+)
1-Mn	Acetate		12.6	-	9.45	250
2-Mn	Acetamide	CF_3-benzoate	25.9		15.35	−15
3-Mn	Acetamide	Acetate	25.9	12.6	16.1	−150
4-Mn	Acetamide		25.9	-	19.42	−465
1-Y	Acetate		12.6	-	9.45	−430
2-Y	Acetoxime	Acetate	25.2	12.6	15.75	−860

EPR spectroscopy

Samples were prepared as solutions (*c.a.* 1 mM) in 1:1 CH_2Cl_2:2-MeTHF and rapidly cooled in liquid nitrogen to form a frozen glass. X-band CW-EPR experiments presented in this study were acquired at the Caltech EPR facility. X-band CW EPR spectra were acquired on a Bruker (Billerica, MA) EMX spectrometer using Bruker Win-EPR software (ver. 3.0). Temperature control was achieved using liquid helium and an Oxford Instruments (Oxford, UK) ESR-900 cryogen flow cryostat and an ITC-503 temperature controller.

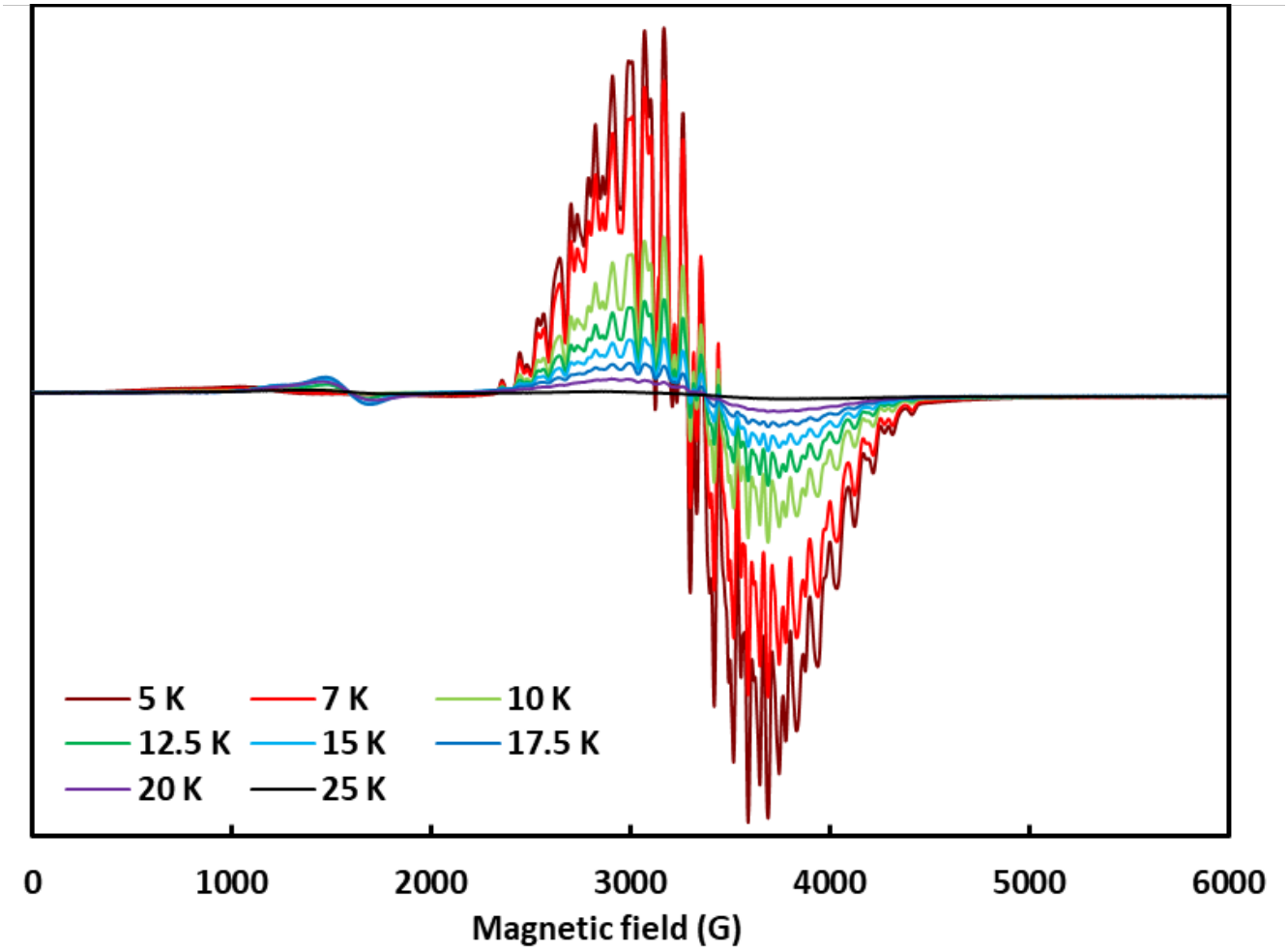

Figure S19. X-band CW-EPR of **4-Mn-ox**. Data acquisition parameters: frequency = 9.366 MHz, power = 2 mW, conversion time = 20.48 ms, modulation amplitude = 8 G. The variable-temperature behavior of **4-Mn-ox** is reminiscent of a recently reported $[LMn^{III}Mn_3{}^{IV}O_4(diamidate)(OAc)]^+$ complex.[2]

References

(1) Qin, C.-J.; James, L.; Chartres, J. D.; Alcock, L. J.; Davis, K. J.; Willis, A. C.; Sargeson, A. M.; Bernhardt, P. V.; Ralph, S. F., An Unusually Flexible Expanded Hexaamine Cage and Its CuII Complexes: Variable Coordination Modes and Incomplete Encapsulation. *Inorg. Chem.* **2011**, *50*, 9131.

(2) Lee, H. B.; Shiau, A. A.; Oyala, P. H.; Marchiori, D. A.; Gul, S.; Chatterjee, R.; Yano, J.; Britt, R. D.; Agapie, T., Tetranuclear [$Mn^{III}Mn_3^{IV}O_4$] Complexes as Spectroscopic Models of the S_2 State of the Oxygen Evolving Complex in Photosystem II. *J. Am. Chem. Soc.* **2018**, *140*, 17175.